

Supporting Information

Morphology Processing by Encapsulating GeP₅ Nanoparticles into Nanofibers toward Enhanced Thermo/Electrochemical Stability

Yaqing Wei,^{†,§} Jiajun Chen,^{†,§} Jun He,^{†,§} Ruihuan Qin,^{†,§} Zhi Zheng,[†] Tianyou Zhai,[†] and Huiqiao Li^{†,§}*

[†] State Key Laboratory of Material Processing and Die & Mould Technology, School of Materials Science and Engineering, Huazhong University of Science and Technology (HUST), Wuhan 430074, Hubei, PR China

[§] Shenzhen Huazhong University of Science and Technology Research Institute, Shenzhen, 518057, Guangdong, PR China

* Corresponding author: hqli@hust.edu.cn; huiqiaoli@gmail.com

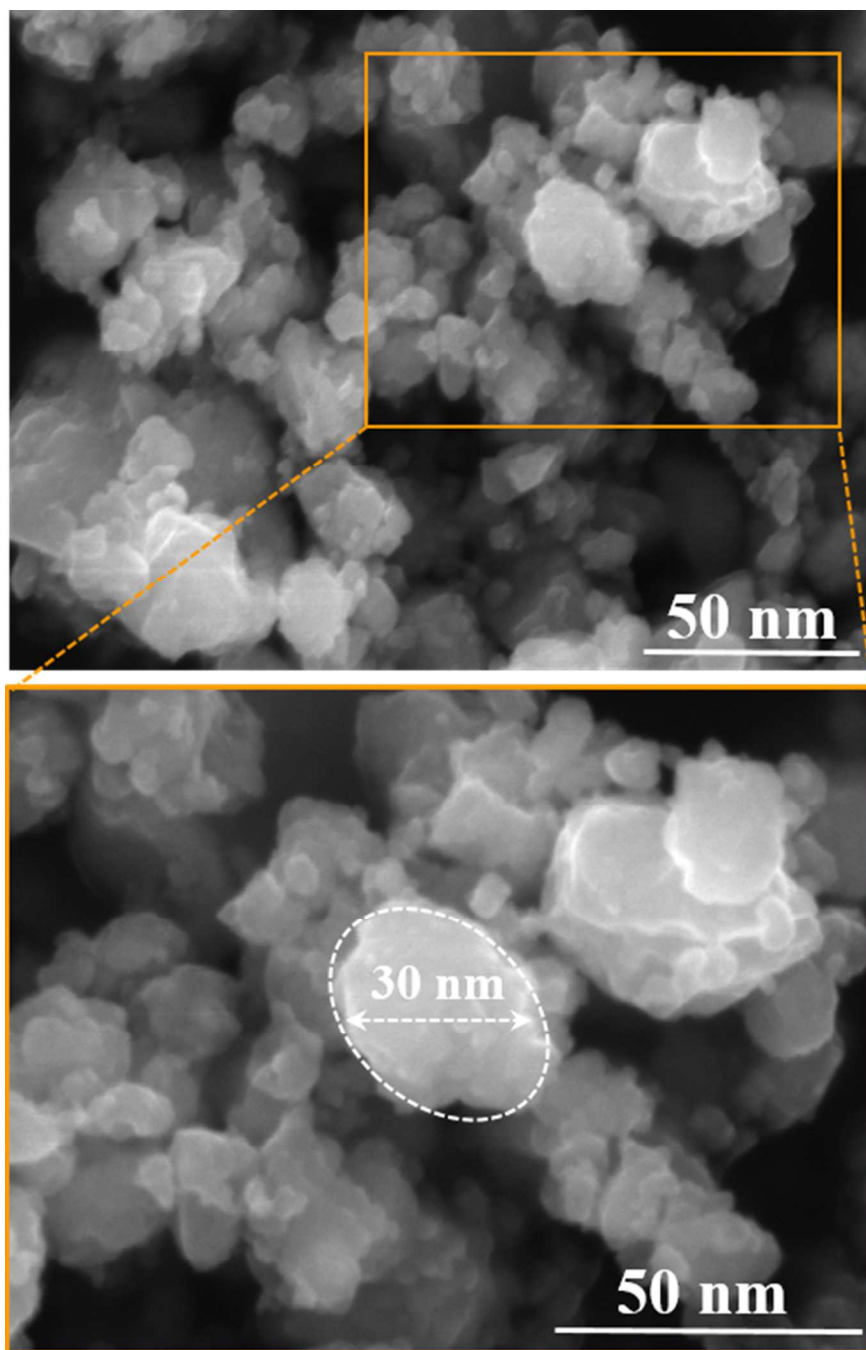


Figure S1. The SEM images of the synthesized GeP₅ powder.

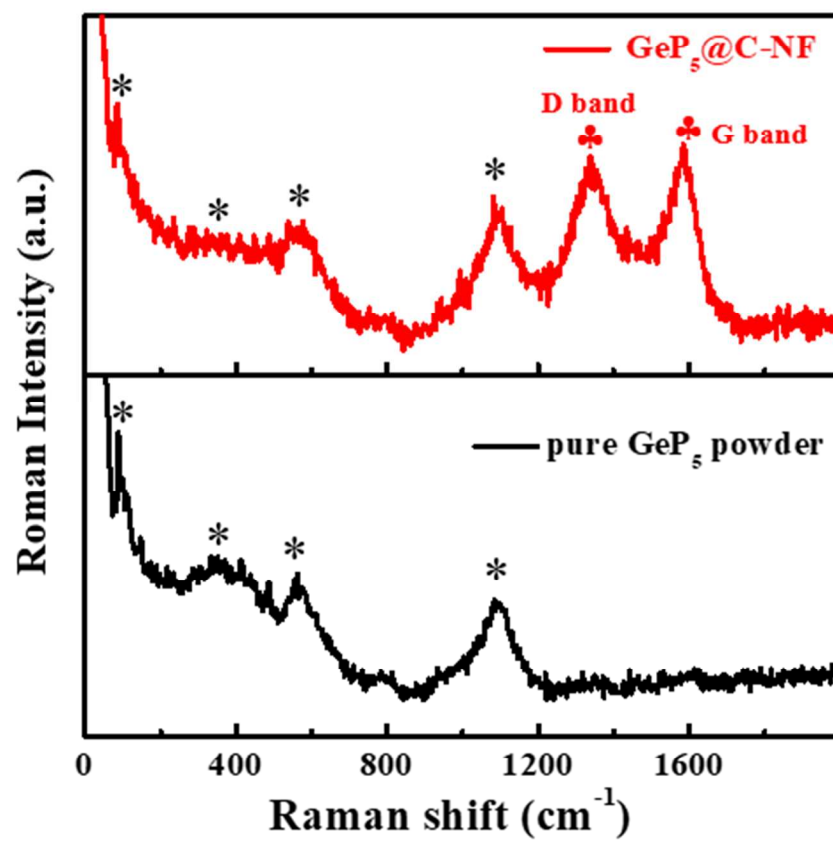


Figure S2. The Raman spectra of the pure GeP₅ powder and GeP₅@C-NF.

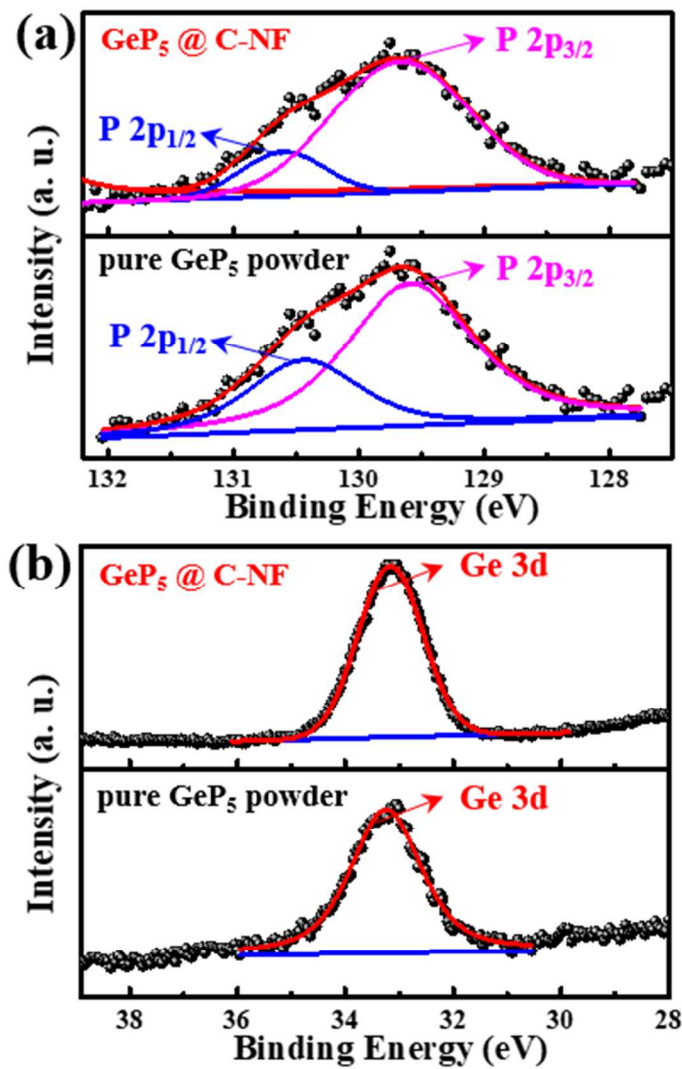


Figure S3. The XPS spectra of the prepared pure GeP_5 powder and GeP_5 @C-NF: (a) P 2p and (b) Ge 3d.

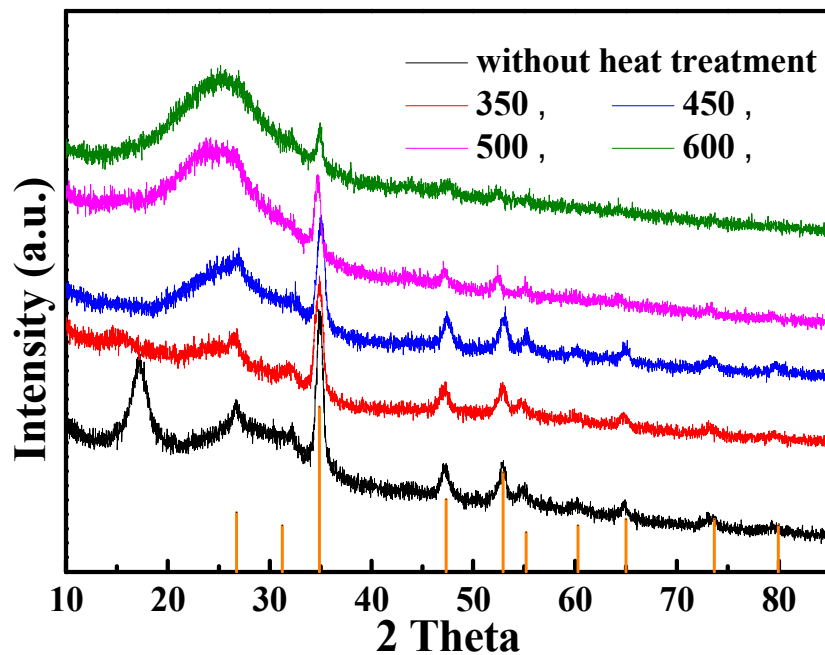


Figure S4. The XRD patterns of the GeP₅@PAN after calcining at different temperatures.

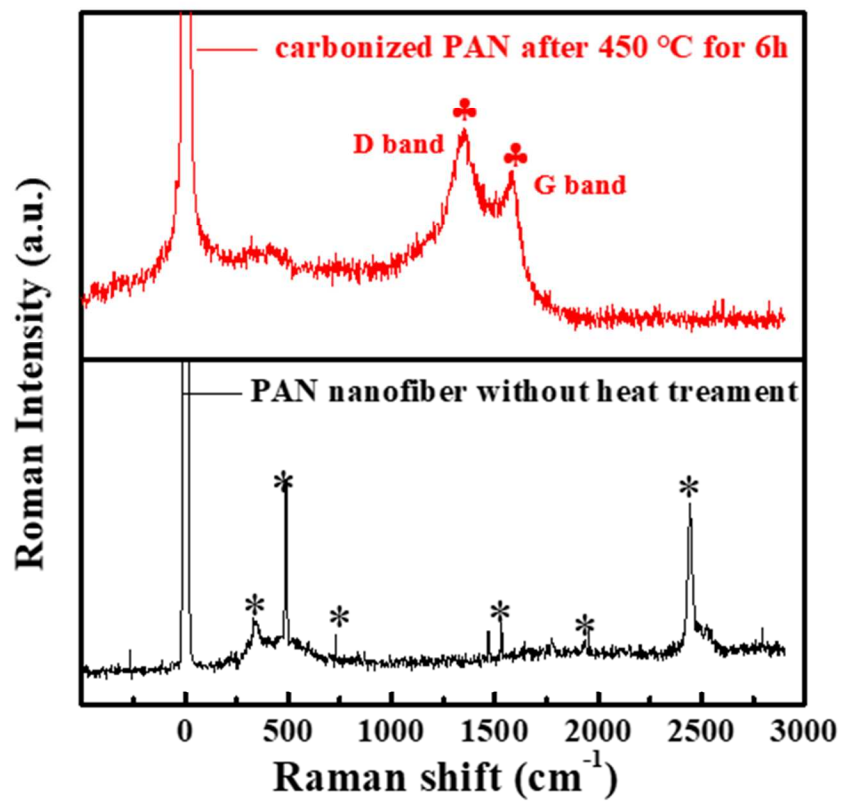


Figure S5. The Raman spectra of PAN precursor without heat and after 450 °C for 6h.

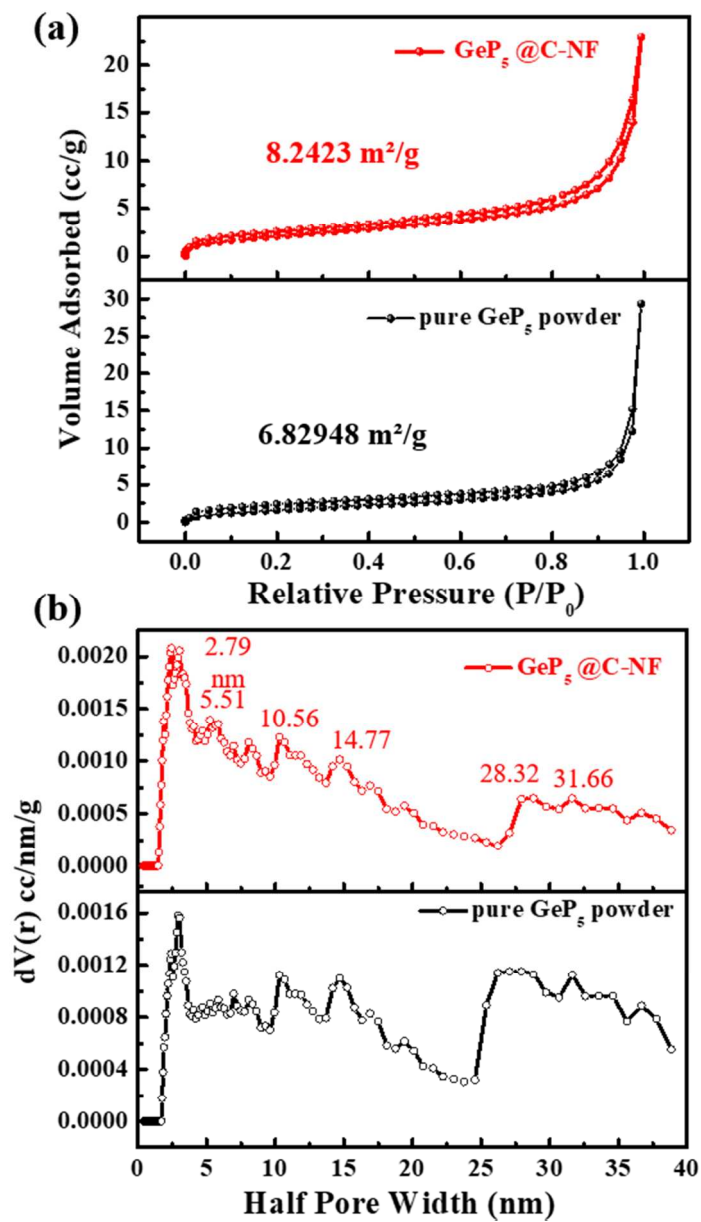


Figure S6. The N_2 sorption isothermal curves (a) and pore size analysis (b) of the pure GeP_5 powder and GeP_5 @C-NF.

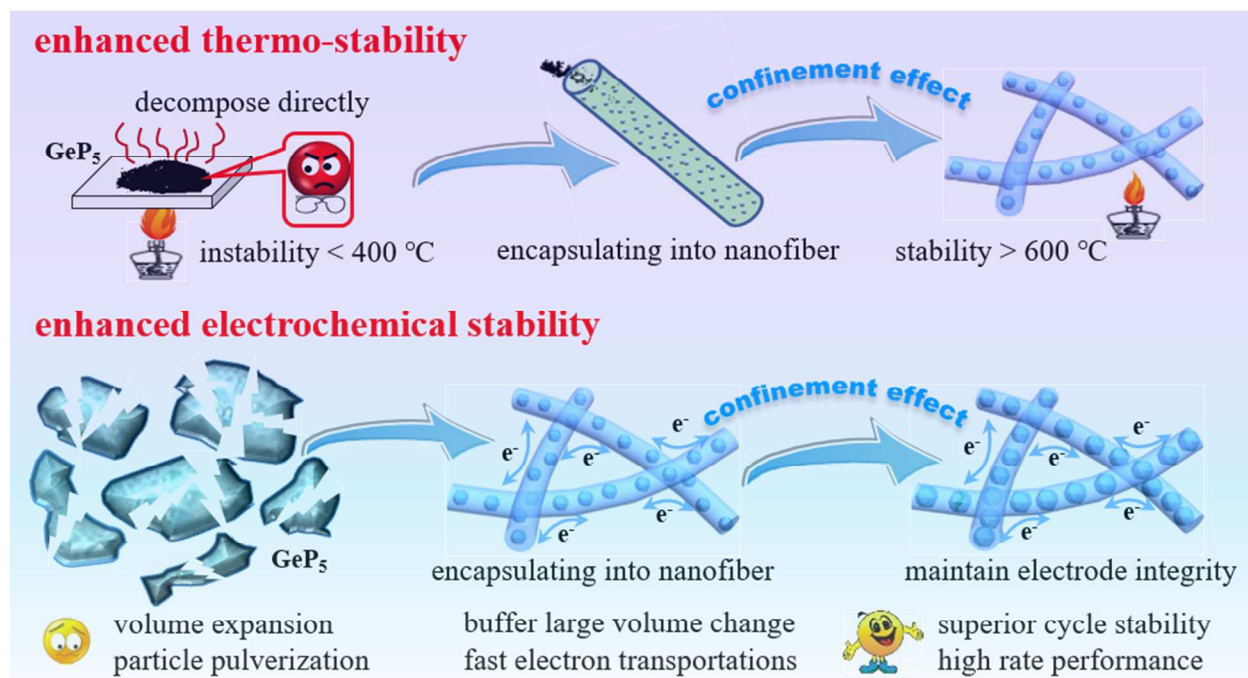


Figure S7. The schematic mechanism illustration of the enhanced thermo/electrochemical stability for the $\text{GeP}_5@\text{C-NF}$.

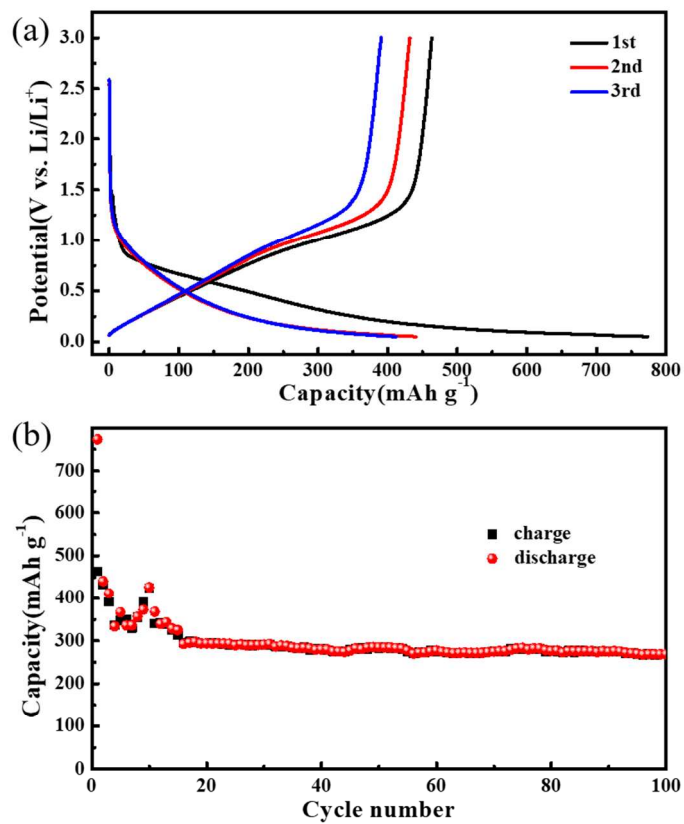


Figure S8. Galvanostatic discharge/charge curves (a) and cycle performance (b) of the carbon matrix.

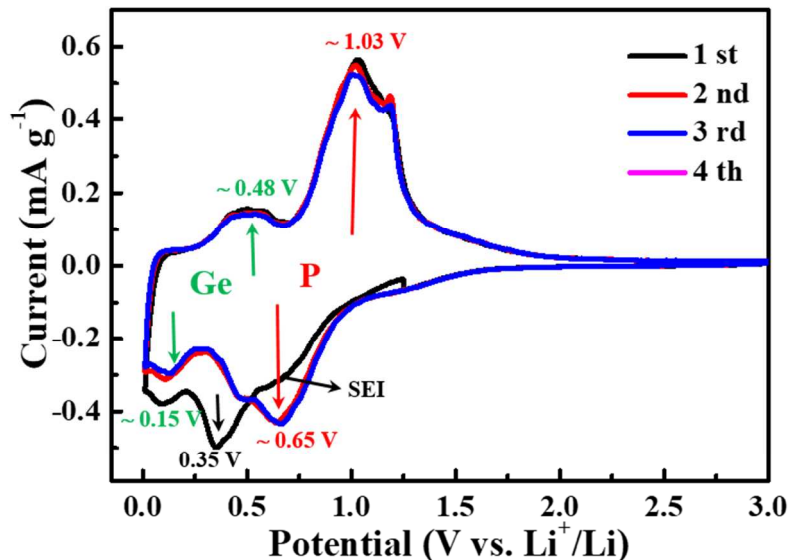


Figure S9. The cyclic voltammetry curves of the GeP₅@C-NF electrode.

During the first cycle, an irreversible small peak for the first reduction at around ~0.65 V was observed, which was principally due to the formation of the SEI film. The following reduction peaks at ~0.35 V and ~0.15 V were associated with the formation of Li₃P and Li₂₂Ge₅ respectively during lithiation. Subsequently, two oxidation peaks were observed in positive scan, which can be assigned to the extraction of lithium from Li₂₂Ge₅ (~0.48V) and Li₃P (~1.03), respectively. In the following cycles, the pronounceable reduction peaks corresponding to Li₃P formation moved to higher potential of ~0.65 V, while the oxidation peaks at ~1.03 were unaffected. This change during the first discharge was probably due to the primary activation of the electrode in the first cycle. By comparing the peak symmetry as well as peak intensity between cathodic and anodic scans, the GeP₅@C-NF electrode exhibited highly reversibility. And the above observations clearly showed that GeP₅@C-NF undergoes synergistic Li-storage of both Ge and P elements.

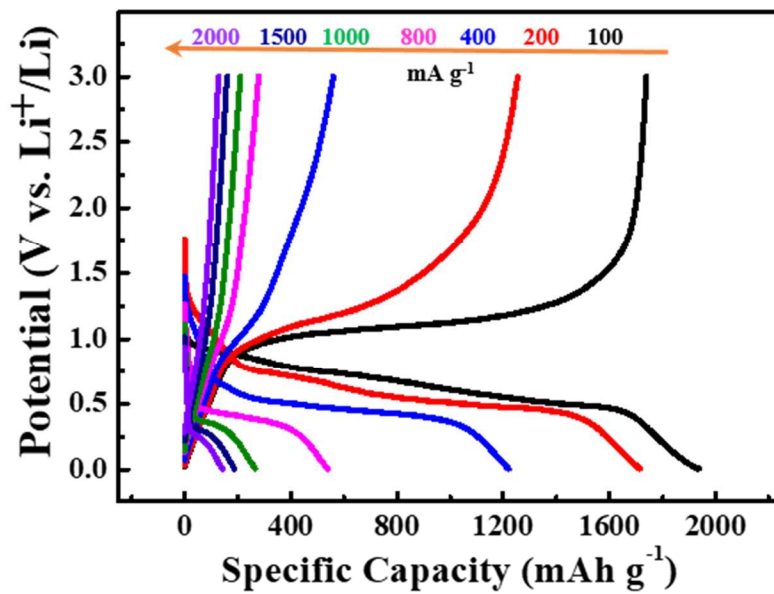


Figure S10. The discharge/charge curves at different current density of the pure GeP₅ powder.

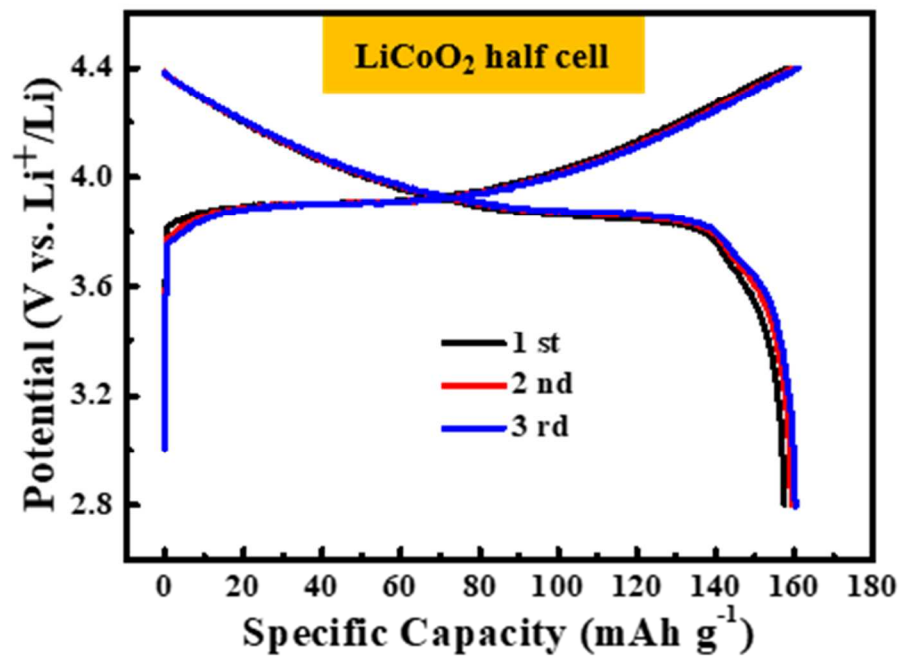


Figure S11. The galvanostatic discharge/charge curves of the LiCoO₂ half-cell.